SAND--89-2268

DE91 000080

SAND89-2268
Unlimited Release
Printed August 1990

COMPARISON OF CALCULATIONS AND IN SITU RESULTS FOR A LARGE, HEATED TEST ROOM AT THE WASTE ISOLATION PILOT PLANT (WIPP)*

Darrell E. Munson
Repository Isolation Systems Division 6346
Sandia National Laboratories
Albuquerque, New Mexico 87185

Kerry L. DeVries
RE/SPEC Inc.
Rapid City, South Dakota 57709

Gary D. Callahan
RE/SPEC Inc.
Rapid City, South Dakota 57709

For Presentation at and Publication in the Proceedings of the
31st U.S. Symposium on Rock Mechanics
Golden, Colorado
June 18-20, 1990

* This paper or article has been accepted for publication in the designated conference proceedings or journal, but may differ from its present form when it is published therein.

Comparison of calculations and in situ results for a large, heated test room at the Waste Isolation Pilot Plant (WIPP)*

Darrell E. Munson
Sandia National Laboratories**, PO Box 5800, Albuquerque, NM 87185

Kerry L. DeVries
RE/SPEC Inc., PO Box 725, Rapid City, SD 57709

Gary D. Callahan
RE/SPEC Inc., PO Box 725, Rapid City, SD 57709

ABSTRACT: The closure measurements from a large scale, heated, in situ experimental room in salt are compared to numerical calculations using the most recent predictive technology, with very good agreement, limited potentially only by the unmodeled roof fracture and separation.

1 INTRODUCTION

The mission of the Waste Isolation Pilot Plant (WIPP) Project is to develop the technology for safe disposal of the radioactive Transuranic (TRU) waste forms generated by the U.S. defense programs. The WIPP facility, now in preliminary operation in anticipation of receipt of small quantities of radioactive waste for experimental purposes, as been constructed in the bedded salt deposits of Southeastern New Mexico. In the existing regulatory context, the requirement is to assure that the potential repository isolates the radioactive waste from the accessible environment and mankind. This requirement means, in part, that the creep closure and waste encapsulation of the salt must be predicted far into the future, a capability which requires a significant development of predictive technology. Very early in the development of the structural prediction technology, it was decided to rely where possible on first principles or, where that was impossible, on laboratory empirical data as the basis for the technology. A series of large scale in situ experiments were fielded at the WIPP specifically to provide a data base for validation of the independently developed prediction technology. In this paper, we present the results of one large scale, heated test as analyzed according to the most advanced predictive capability.

2 IN SITU EXPERIMENT

The underground workings of the WIPP facility were excavated into the bedded salt layers at a depth of about 659 m below ground surface. A portion of the underground facility is devoted to thermal/structural in situ tests. These experiments have been heavily instrumented to measure room closures, ground displacements, stresses during and after mining, and temperatures as heating occurred [Matalucci et al., 1982]. One of

*Work supported by US Dept. of Energy (DOE), contract DE-AC04-76DP00789.
**A US DOE facility.

the major thermal/structural tests (Room B) consists of a long (93.3 m) instrumented room with a square cross-section (5.5 m by 5.5 m) [Munson et al., 1989a]. As shown in the Figure 1 elevation, this room has electrically heated canisters (0.30 m diameter by 3.0 m long) placed in evenly spaced boreholes (0.41 m diameter by 4.9 m deep) in the floor along the room center line. These heaters, each with about 1.8 kW of power, were placed on 1.52 m centers to give a linear heat load of 1.18 kW/m over the central 41.2 m of the room.

The room was excavated by continuous miner in three major passes and several trims beginning May 4 and ending June 5, 1984. Closure measurements were made during the excavation process from points emplaced within 1.0 m of the mining face and within 1.0 hr of the mining of that location [Munson et al., 1987]. These manual mining sequence measurements were continued until the permanent remote recording instruments were installed. The room was heavily instrumented with remote gages, including vertical and horizontal closure gages, multipoint extensometers extending up to 15.1 m into the surrounding salt, and stress meters. Three different thermocouple arrays were used to monitor the temperature conditions in the room: (1) one monitored the interior canister temperatures, (2) one monitored the near-field temperatures in the immediate vicinity of the canisters, and (3) one monitored the far-field temperatures in the salt around the room. In addition, power and flux meters monitored the heater conditions. When completed, over 1160 gages were fielded in this experimental room.

The test room operated in an unheated condition, intentionally, until March 23, 1985, to give a baseline room response for comparison to other, similar experimental rooms. Part of this time was also necessary to permit emplacement of the heaters and construction of insulated doors at the ends of the room. When the heaters were activated, the doors were closed and access to the room was restricted to decrease room heat loss through the circulating mine ventilation air. During the course of the experiment, (1) the room became too hot (approaching 52°C) for humans to work in except for limited times, (2) the room deformation was pronounced, and (3) the immediate roof eventually developed significant separations. On February 7, 1988, about 1374 days (3.74 yrs) after the start of excavation, of which 1020 days (2.79 yrs) were heated, the experiment was interrupted to permit ventilation and recovery of waste package simulation heater tests from the room.

A significant feature of this experiment is the heating. Because the creep of salt is a thermally activated process, a modest increase in temperature produces a marked acceleration in room closure rate. Moreover, closure results from an unheated room (Room D) of identical dimensions are available for comparison [Munson et al., 1989b]. This comparison, shown in Figure 2, clearly illustrates the influence of heating on room response. Prior to heating, on day 354, the two rooms show essentially identical behavior; but the measured closure of Room B accelerated to a much higher closure rate immediately after the heaters were activated. Total Room B vertical closure at the end of the test data reported here was approximately 1.0 m.

3 CALCULATIONS OF ROOM B RESPONSE

Numerical simulation of the thermal and mechanical response of Room B is especially challenging because it involves a very complex thermal situation in which heat is lost through normal heat transport across insulated doors at the room ends and because it involves the previously untested thermal activation parameters of the constitutive model.

3.1 Thermal calculations

Accurate thermal calculations are very critical for the structural evaluation of large scale heated experiments in salt. Temperature changes affect the structural calculations in two ways: (1) thermal expansion induces loads which can alter the stress field even beyond the region where the temperatures are changing and (2) the creep response of salt is influenced because the creep strain rate is temperature dependent. The actual setting of the experiment must be modeled carefully to account for heat losses from the room. Normal mine ventilation air with an average velocity of 0.9 m/s circulated past the entries to Room B. This air was prevented from circulating through the room by insulated doors. However, a marked heat loss apparently occurs through the doors into the mine ventilation air [Munson et al., 1989a]. Previous thermal calculations of heated experiments at the WIPP have accounted for the heat loss through the access drift doors by reducing the thermal load [e.g., Munson et al., 1988]. Reducing the thermal load in the calculation for this experiment in a similar manner was deemed inappropriate because the magnitude of the temperatures in the heater area would be artificially low. In fact, heat is lost from below the floor by conduction through the salt to the room periphery where convective and radiative processes can become important. Heat transport occurs by convection along the room periphery and conduction into the salt at the room ends. Additional conduction and infiltration losses occur through the room doors and into the ventilation air. As a result, the most suitable simulation for heat loss from the Room B test was thought to be a time dependent heat sink in the room that varied with the temperature rise.

In the thermal model, all external boundaries were assumed to be adiabatic and were shown to be sufficiently removed that they did not affect the calculation during the time of interest. Heat transfer in the salt was modeled with a nonlinear thermal conductivity given by:

$$\lambda = \lambda_{300}(300/T)^{\gamma}$$

where λ is the conductivity, T the temperature in Kelvin, and λ_{300} and γ are material constants given in Table 1 [Krieg, 1984]. Also included in the table are the values for specific heat (C_p), coefficient of thermal expansion (α), and density (ρ). Heat transfer in the salt is by conduction. Radiative and convective heat transfer between room surfaces within the room was adequately simulated using an "equivalent" conductive material, with parameters given in Table 1.

Thermal loss from the room was modeled by a convective boundary at the room surfaces using Newton's law of cooling:

$$\tilde{q} \cdot \tilde{n} = h(T - 300)$$

where $\tilde{q}$ is the thermal flux vector, $\tilde{n}$ is the outwardly normal unit vector, h is the convective heat transfer coefficient, and T the surface temperature. The convective boundary acts as a heat sink whenever the temperature on the room surface exceeds the initial 300 K temperature. Thus, as the room surface temperature rises, the rate of heat loss increases. Because the convective heat transfer coefficient was unknown, it was adjusted prior to any structural calculation until a suitable value (0.51 W/m^2K) was determined to give agreement with the measured temperatures.

The thermal calculations were made with the two-dimensional heat

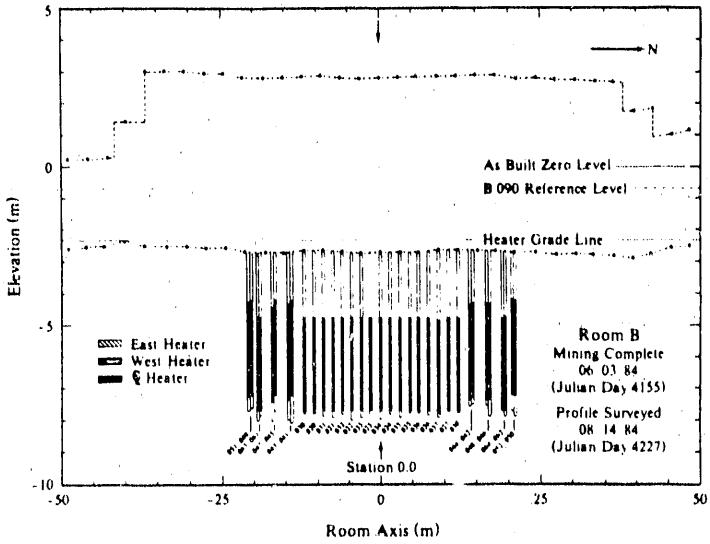

Figure 1. Elevation of Room B, with heaters.

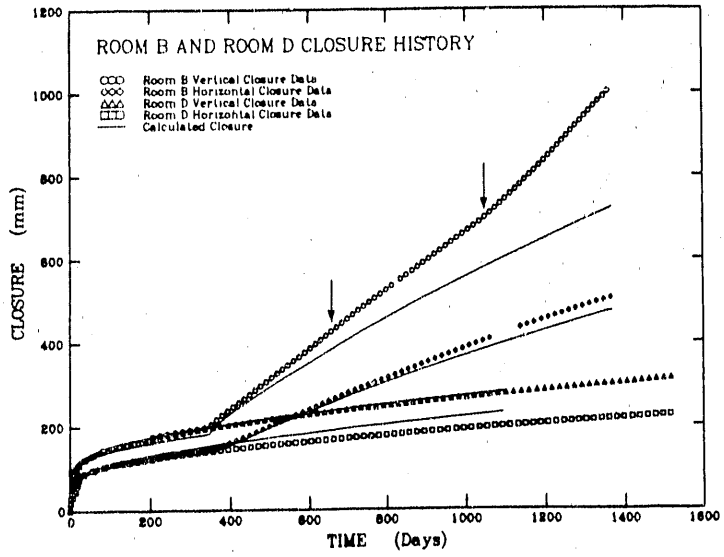

Figure 2. Predicted and measured Room B and D closures.

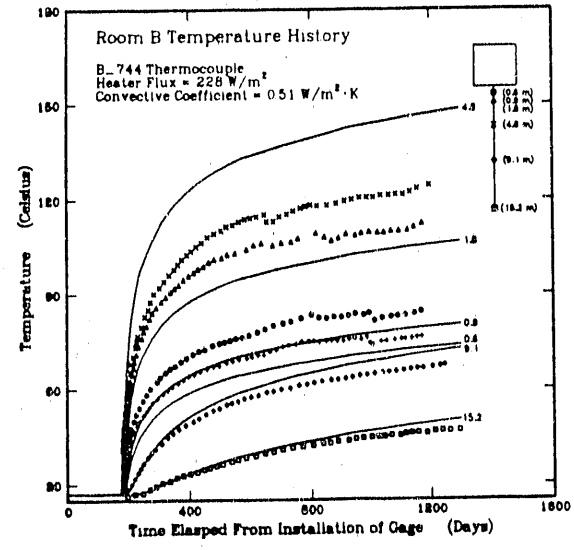

Figure 3. Measured and calculated floor temperatures.

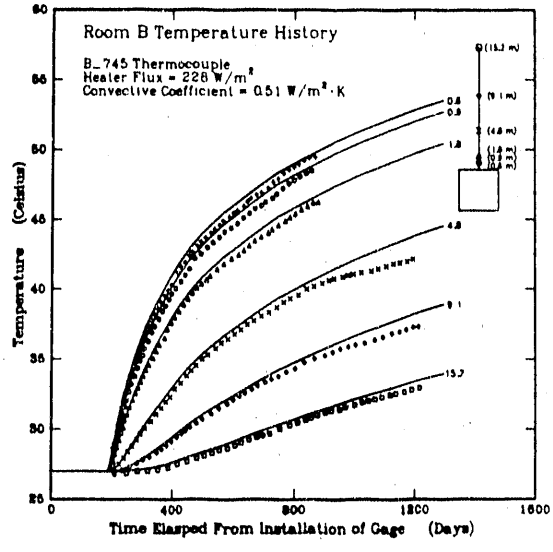

Figure 4. Measured and calculated roof temperatures.

Table 1. Thermal parameters

Material	C_p J/kg K	α 1/K	λ_{300} W/m K	γ	ρ Mg/m^3
Halite	862	45.E-6	5.4	1.14	2.3
Anhydrite	733	20.E-6	4.7	1.15	2.3
Polyhalite	890	24.E-6	1.4	0.35	2.3
Air (Equivalent Thermal Material)	1000	-	50.0	0.00	1.0

transfer code SPECTROM-41 [Svalstad, 1989]. These calculations are compared to measured far-field temperatures obtained from thermocouple gages oriented vertically downward in the floor midway between two canister heaters and thermocouple gages oriented vertically upward in the roof. Because of the discrete heater locations, a situation which is not modeled by the two-dimensional calculations, the calculations will show discrepancies when compared to the measured floor results. These discrepancies will be less pronounced at distances further from the heaters, i.e, at greater depths into the salt. Consequently, in Figure 3, the calculated temperatures, while close, do not exactly match the salt temperatures just below the room. In fact, we have intentionally left the calculated near floor temperatures higher than those measured in an attempt to average the higher temperatures that occur near the heaters with those found midway between heaters. The deeper salt temperatures are in close agreement, as necessary, because at these depths the discrete heater effects are no longer apparent.

Temperatures in the ribs and roof are quite uniform, as expected, because the discrete heater effects are well removed from these locations. As Figure 4 shows, the comparison between calculated and measured temperatures of typical thermocouple unit in the roof is excellent. Although not shown, rib units are calculated equally well.

3.2 Structural response

Room structural response is based on the multimechanism steady state, workhardening and recovery transient creep model developed by Munson and Dawson [1982], as recently modified by Munson et al. [1989b]. Based on the creep mechanism map, we believe that of the three controlling mechanisms proposed in the complete model at least the two high temperature mechanisms are active for the temperatures and stresses experienced in Room B. This is in contrast to the constant temperature experiment of Room D [Munson et al., 1989b], where probably only the low temperature creep mechanism is active.

In the current calculations, the stratigraphy and material parameters used for the earlier Room D calculations [Munson et al., 1989b] were adopted with only minor changes. The creep temperature dependence is basically that initially determined by Munson and Dawson [1982]. Additionally, the coefficient of friction of 0.2 between the bedded stratigraphic layers was also adopted unchanged. The flow potential was the Tresca maximum shear stress criterion.

The calculation differs from the earlier Room D calculations in that the four anhydrite layers in the WIPP stratigraphy, including a thick anhydrite bed about 6.8 m below the common floor elevation of Room B and Room D, were modeled here as a Drucker-Prager material rather than

as salt. The anhydrite was considered to be isotropic and elastic until yield occurs. Once yield is reached, plastic strain accumulates. Yield is governed by the Drucker-Prager function:

$$Y = a I_1 + \sqrt{J_2} - C$$

where J_2 is the second deviatoric stress invariant, I_1 the first stress invariant, and C and a are constants. Material parameter values are C = 1,350 MPa and a = 0.450.

The thermal/structural calculation was made using the two-dimensional finite element code SPECTROM-32 [Callahan et al., 1989]. The results of this calculation appear in Figure 2. Agreement between calculated and measured Room B closure is considered to be very good, with an underprediction of horizontal and vertical closures of about 4% and 15%, respectively, at 1000 days. The discrepancy in the horizontal closure is probably the result of uncertainty in values of the high temperature creep parameters. However, the large discrepancy between the calculated and measured vertical closure is believed to be a direct consequence of fracture and separation in the immediate roof. Where roof separations do not occur, as in Room D, the vertical closure prediction is in good agreement with the measured closure. Because separations do not occur in the ribs, the prediction of horizontal closures in both Room B and Room D are quite accurate.

3.3 Roof failure process

At this point in the development of a predictive technology, only the continuum deformation process of creep has been investigated. Although failure is certainly possible in the normal underground situation of convergent room closure, the compressive stress field extending in depth around the room suppresses the onset of fracture. However, local strain concentrations may accumulate near the room surface, caused by stress perturbations induced by room geometry, bedding interfaces, and clay stringers. As a consequence, local failure sites can also nucleate and grow at the strain accumulation locations in the immediate vicinity of the room surface. These failures can be either in the massive salt layers, in the interbeds between salt layers, or at clay stringer concentrations. With time these failures can grow to form relatively thin fracture or separation slabs in the immediate surface of the room.

Because of the very large displacements around Room B, one would expect such failures to occur. In fact, direct evidence of roof failure by separation is seen in the vertical closure data. After about 1000 days, some vertical closure gages, but not all, show marked increases in the apparent closure rate. This increase correlates with visual observations of major cracks appearing along the length of the room roof during March 1988 (roughly day 1045). While the exact nature of the separation process is not known, it is likely that the localized strain damage accumulation at the plane of imminent failure is a source of additional vertical displacement. However, because such slowly accumulated strains would be indistinguishable from the massive salt creep deformation, they may be undetectable. In fact, a "drummy" roof with small cracks was observed as early as February 1987 (roughly day 650) during the hammer soundings common to mine safety inspections, although no associated closure accelerations were obvious at that time.

After visible separation occurs, the closure and extensometer data can be analyzed in terms of the slab motions. In Figure 5, a room cross section shows the configuration of the roof at late times. Initial

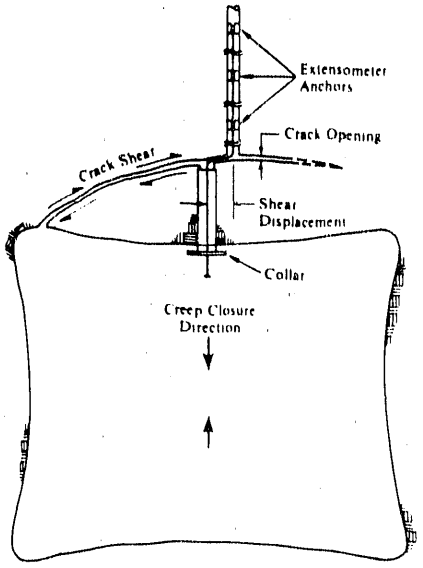

Figure 5. Schematic of roof crack separation and shear.

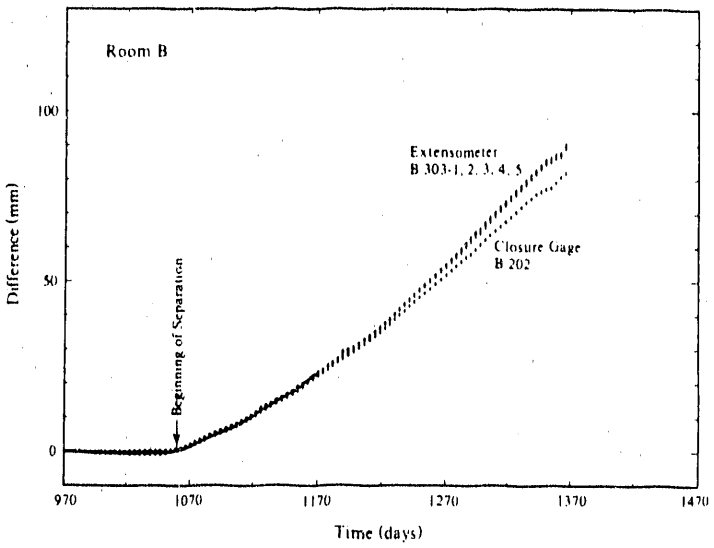

Figure 6. Difference in measured and extrapolated displacements.

separation has progressed until a fracture has developed through the slab and into the room on one side of the separation. The figure also illustrates that the slab motions can have both vertical crack opening (separation) and horizontal crack offset (shear) components. The wire extensometers that span the failure region measure the sum of the crack opening and shear; whereas, the closure gage measures only the crack opening displacement.

After beginning of separation, we can take the difference between a reasonable extrapolation of expected creep deformation and the measured curve. The results in Figure 6 show two things. First, all of the extensometer gages in the hole, with depths ranging form 0.9 to 15.1 m, show the same increased rate which indicates separation occurs only between the extensometer collar and the shallowest anchor. As a result, we know the slab thickness is less than the shallowest anchor location (0.9 m). Second, the increased displacement measured by the closure gage is less than that measured by the extensometers, a situation which causes a major defect in the displacement summation across the gage station. For the station of Figure 6, the roof slab has a separation of about 82 mm and a shear displacement of about 8 mm at day 1250. Because

of the failure process, the separation to shear ratio will in general be non-uniform throughout the room.

It should be remembered that slab motions are not directly related to the massive salt creep process. In fact, once separation occurs, the slab behaves initially as a clamped beam, with end loading, until fracture at one side makes it into a nearly stress-free member hinged on one side. This causes formation of an effective new room surface behind the unstressed slab. Because the slabs are essentially free bodies of such small thicknesses compared to the volume of creeping salt, the total room closure time is basically unaffected by the formation of such slabs. The massive salt beyond this new surface continues to obey the normal creep constitutive law.

4 SUMMARY

The results show that the previously developed constitutive model for prediction of creep closure behavior can be extended from unheated conditions to the heated conditions of Room B to give very good agreement (15%, including cracking, for vertical and 4% for horizontal closures) over nearly 1020 days of heating. Although the creep response controls the room closure with time, the gages measure increases in closure rates because of local failures near the immediate room surface. In Room B a relatively thin (<0.9 m) slab forms in the roof.

REFERENCES

Matalucci, R.V., C.L. Christensen, T.O. Hunter, M.A. Molecke, and D.E. Munson 1982. Waste Isolation Pilot Plant (WIPP) research and development program: In situ testing plan, March 1982, SAND81-2628, Sandia National Laboratories, Albuquerque, NM.

Munson, D.E. and P.R. Dawson 1982. A transient creep model for salt during stress loading and unloading, SAND82-0962, Sandia National Laboratories, Albuquerque, NM.

Krieg, R.D. 1984. Reference stratigraphy and rock properties for the Waste Isolation Pilot Plant (WIPP) Project, SAND83-1908, Sandia National Laboratories, Albuquerque, NM.

Munson, D.E., T.M. Torres and R.L. Jones 1987. Pseudostrain representation of multipass excavations in salt, Proc. 28th U.S. Symp. Rock Mech., A.A. Balkema, Boston, MA: pp. 853-862.

Munson, D.E., T.M. Torres and R.L. Jones 1988. Results of a large, in situ, heated axisymmetric pillar test at the Waste Isolation Pilot Plant (WIPP), Proc. 29th U.S. Symp. Rock Mech., A.A. Balkema, Brookfield, MA: pp. 641-652.

Callahan, G.D., A.F. Fossum and D.K. Svalstad 1989. Documentation of SPECTROM-32: a finite element thermomechanical stress analysis program, RSI-0269, RE/SPEC Inc., Rapid City, SD.

Munson, D.E., R.L. Jones, D.L. Hoag, J.R. Ball, R.M. Clancy and S.V Petney 1989a. Overtest for simulated defense high-level waste (Room B) in situ data report (May 1984 - February 1989), SAND89-2671, Sandia National Laboratories, Albuquerque, NM.

Munson, D.E., A.F. Fossum, and P.E. Senseny 1989b. Approach to first principles model prediction of measured WIPP in situ room closure in salt, Proc. 30th U.S. Symp. Rock Mech., A.A. Balkema, Brookfield, MA: pp. 673-680.

Svalstad, D.K., 1989. Documentation of SPECTROM-41: A finite element heat transfer analysis program, SAND88-7122 (contractor report), Sandia National Laboratory, Albuquerque, NM.

END

DATE FILMED

11 / 06 / 90